THIS MANUSCRIPT HAS BEEN SUBMITTED TO PLOS ONE. PLEASE NOTE THE MANUSCRIPT HAS YET TO BE FORMALLY ACCEPTED FOR PUBLICATION.

A multicriteria decision analysis framework for generating baseline virtual weather stations in Zimbabwe

Tinetariro Wesley Chikati[1*], Tambudzai Theresa Ngatiane[2]

[1]Zimbabwe Meteorological Services Department, Belvedere, Harare, Zimbabwe

[2] Department of Geospatial Science, National University of Science & Technology, Bulawayo, Zimbabwe

*Corresponding author. Email: tinechik@gmail.com

Abstract

In this study, we generate baseline Virtual Weather Stations (VWS) in locations with minimal atmospheric noise by avoiding two major surface factors known to cause noise in remotely sensed weather observations. The study also proposes an improvement to the spatial coverage of Zimbabwe's weather observation network through the identification of environmentally suitable locations for virtual station deployment, where physical infrastructure could also be placed. A geospatial multi-criteria decision analysis approach was applied, using a weighted combination of Terrain Ruggedness Index (TRI) and proximity to large-scale water bodies, constrained by distance from existing physical weather stations, to determine optimal locations. Sixty-three Virtual Weather Station locations were generated to complement the existing network of 45 active physical weather stations. To maximise coverage and reduce duplication of observations, the virtual stations were strategically located beyond the influence zones of existing stations. The average nearest-neighbour distance of 59.68 km indicated a well-balanced and spatially efficient network. Network representativeness was further assessed across Zimbabwe's Agro-Ecological Zones (AEZs). The results showed that Regions IV and Va received the highest number of virtual stations. Conversely, the existing physical weather station network was concentrated within smaller AEZs, leaving larger regions relatively underrepresented. Environmental validation demonstrated that the optimised network occupied significantly less rugged terrain than a randomly generated control network. The VWS locations recorded a mean Terrain Ruggedness Index of 10.23 m and a median of 9.33 m, compared to 53.79 m and 29.82 m for the random network. A Mann–Whitney U test confirmed that these differences were statistically significant ($U = 425.00$, $p < 0.001$). Blind spot analysis further revealed that integrating the virtual network with existing stations substantially reduced observational gaps across Zimbabwe, demonstrating potential to improve weather monitoring in regions with sparse physical monitoring infrastructure.

Keywords: terrain ruggedness index, observational blind spot, multi-criteria decision analysis, network optimisation, satellite rainfall retrieval

Introduction

The accuracy and precision of weather forecasting and disaster risk management are mostly rooted in the consistency and spatial density of meteorological observations (1). High-quality, real-time data are the informants of a nation's climate monitoring system. In the current era of high climate unpredictability, the ability to monitor microclimates has moved from a scientific luxury to a necessity for water resource management and the population's food security. While this importance is evident, a wide data gap exists across much of the developing world (2). In Zimbabwe, the physical network of 45 weather stations is sparse or concentrated in specific places, leaving large parts of the country, particularly remote areas, unmonitored. At the same time, building a dense physical network is logistically and financially impossible, as the stations can be vandalised in remote areas while also being expensive (3). This reliance on a fragmented network creates significant challenges for providing localised climate advisories, as the gaps between physical stations often cover diverse ecological zones.

According to the World Meteorological Organization (WMO), for flat regions, there should be a weather station every 600–900 km², and every 250–575 km² in complex terrain (4), but Zimbabwe's station density falls far short of this benchmark, leaving many areas unobserved. While satellite datasets provide complete spatial and temporal coverage, their utility is diminished by errors arising from atmospheric interference when recording various elements. To overcome atmospheric interference, different bias correction schemes are used to remove the errors associated with remote sensing, using in-situ data from physical instruments (5) and (6) highlighted that the use of bias correction can improve the representativeness of satellite data by roughly 30%. However, not all grids within satellite imagery are equally biased, as they are influenced by different environmental factors. As a result, a method is needed to identify pixels or areas where errors are minimal, that is, where the environment offers a clearer atmospheric window for electromagnetic radiation to propagate freely between the target and the space-borne sensors.

To bridge the station density gap and identify pixels subjected to minimal environmental interference, the concept of a Virtual Weather Station (VWS) is introduced. A VWS has traditionally been employed as a computational alternative to physical infrastructure. In its most basic form, a virtual station is a point with synthetic data generated through the interpolation of variables from the sensors at surrounding physical stations (7). However, traditional VWS models often suffer from interpolation bias, where a virtual point inherits the anomalies of the nearest physical station from which its data was interpolated (8). For example, the cooling effect of a large lake, or barometric pressure spikes caused by high altitude.

Considering these limitations, this paper provides a non-traditional definition of Virtual Weather Stations (VWS). Distance-based algorithms like Kriging usually fail in hydrologically and topographically complex environments, where interpolation introduces bias (9). Instead of treating virtual stations as simple arithmetic gap-fillers generated from such spatial interpolation, this study defines them as baseline virtual stations, whose placement is optimised using a Multi-Criteria Decision Analysis (MCDA) to identify environmentally stable locations. By integrating geospatial constraints and masking the influence of large-scale water bodies and topographic ruggedness, the algorithm selects radiometrically and geographically stable pixels. Avoiding these zones is critical, as hydrological and topographic phenomena severely alter remotely sensed signals (10). Ultimately, this study also validates the VWS network for environmental and spatial efficiency, providing a scalable, cost-effective framework for optimising national meteorological observation networks in support of Zimbabwe's developmental and climate resilience goals.

Materials and methods

Study area

Fig 1 shows the study area, Zimbabwe, a landlocked country located in Southern Africa between northings 15°–23° and eastings 25°–34°. Zimbabwe is made up of ten administrative provinces and seven Agro-Ecological Zones (AEZs), covering a total land area of approximately 390,757 km² (11). Zimbabwe's elevation ranges from a minimum of 162 m above sea level in the low-lying Zambezi and Save valleys to a maximum of 2,500 m in the eastern highlands. This topographic gradient influences temperature patterns and national rainfall distribution, especially in mountainous regions where satellite rainfall retrieval uncertainty is often high (12). Major inland water bodies include Lakes Kariba and Chivero, and dams such as Manyame and Mutirikwi. These water bodies influence local atmospheric moisture conditions and may introduce artefacts in remotely sensed precipitation products due to mixed water and land pixel effects (13). The country's weather is monitored by a network of 45 weather stations distributed across the country. Relative to Zimbabwe's total land area, this corresponds to an average station density of approximately one station per 8,314 km².

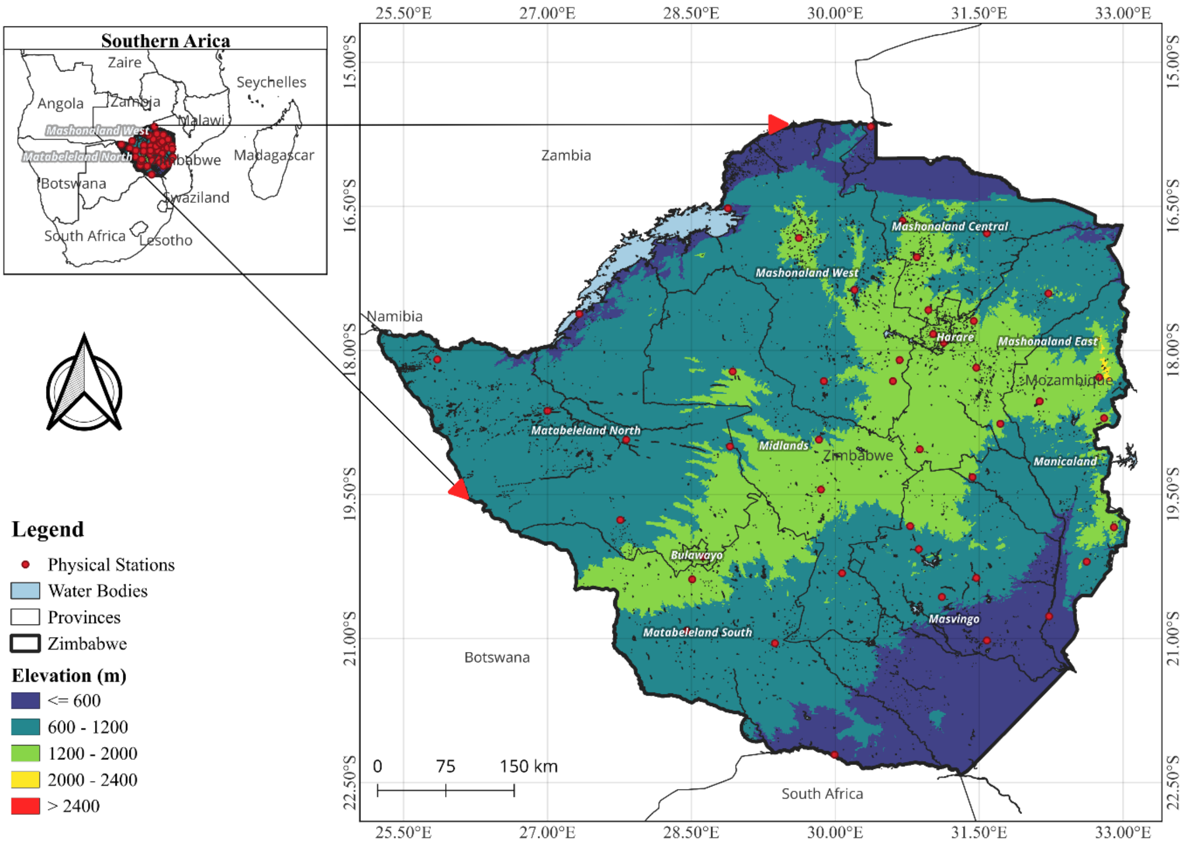

Fig 1. Location of the study area, showing Zimbabwe's ten provinces, manned weather stations (red dots) and elevation

Datasets

Four datasets were used to generate the VWS. These datasets provided the criteria and constraints required for optimised VWS placement. Coordinates for 45 weather stations were obtained from the Meteorological Services Department of Zimbabwe (14). The station coordinates were used as spatial reference points for generating the virtual stations. The Digital Elevation Model (DEM) was obtained from OpenTopography (15). The DEM was used to derive Zimbabwe's terrain characteristics, which were incorporated into the MCDA to identify geographically stable regions with low terrain-induced satellite retrieval bias. Water body polygons were acquired from OpenStreetMap Waterways (16), and their boundaries were used to create exclusion buffers, as mixed land–water pixels can introduce satellite data retrieval bias. Zimbabwe's Agro-Ecological Zones (AEZs) (17) were additionally incorporated to ensure that the generated VWS network captured the major climatic gradients across the country.

Generation of the virtual stations

MCDA was implemented to identify geographically stable VWS locations suitable for satellite rainfall extraction in Zimbabwe. All input datasets were standardised by reprojection to a common coordinate reference system and resampled to a uniform spatial resolution. Two environmental criteria were used: proximity to water bodies and terrain ruggedness. These criteria were further constrained by proximity to existing physical weather stations.

Terrain ruggedness index

The DEM was used to calculate the Terrain Ruggedness Index (TRI) (18). This index quantifies local terrain variability based on the altitude differences between neighbouring pixels. Low-ruggedness zones were considered more suitable for VWS placement, as smoother terrain reduces localised weather variability. TRI was calculated as:

$$TRI = \sqrt{\sum_{i=1}^{n} (x_i - x_{centre})^2} \quad (1)$$

where: x_{centre} is the elevation of the central pixel and x_i is the elevation of neighbouring pixels. The TRI was then normalised to transform the values into a common scale between 0 and 1. The normalisation was done as:

$$TRI_{norm} = \frac{TRI - TRI_{min}}{TRI_{max} - TRI_{min}} \quad (2)$$

where: TRI is the original terrain ruggedness value, TRI_{min} is minimum TRI value and TRI_{max} is the maximum TRI value.

Proximity to water bodies and physical stations

This criterion was used because abrupt emissivity transitions near water bodies can cause radiometric errors in remotely sensed precipitation datasets (19). Euclidean distance from water bodies was calculated, and areas farther from water bodies were assigned higher suitability scores. To maintain climatological representativeness between the national grid and the VWS, distance from existing physical weather stations was also considered. Euclidean distance to the 45 operational weather stations was determined, and areas located within 30 km of the PWS were given higher suitability scores to ensure they were representative of existing climatological monitoring conditions while avoiding clustering.

Weighting structure and framework validation

Using the Analytical Hierarchy Process (AHP) (20), the weighting structure assigned greater importance to terrain stability and water body distance, as these have the strongest influence on satellite rainfall retrieval stability. The secondary constraint was proximity to PWS, to enhance the representativeness of the VWS. The final suitability surface was ranked according to suitability, and the virtual station locations were generated at the most stable locations, for subsequent rainfall extraction and validation analyses. Terrain ruggedness and distance to water bodies were assigned 75 and 25 as the percentage weights respectively.

Macro scale network proportionality and micro scale dispersion

A proportionality test was conducted to ensure the generated VWS network did not skew observational weight toward specific regions. To evaluate whether the frequency of VWS was proportionate to the area of each agro-ecological zone, a Chi-Squared Goodness of Fit test was used, ensuring the network was climatologically representative. To verify that localised data redundancy was eliminated, the Average Nearest Neighbour (ANN) distance between stations was determined. The minimum, maximum, and average separation distances between stations were determined, with the framework set to use a threshold of 50 km between neighbouring stations. This ensured that no two stations possessed overlapping observational footprints.

Environmental constraint validation

To prove the efficacy of the MCDA, an independent control experiment was designed. A random control group with a sample size equivalent to the generated VWS was generated within the national boundary. Using both the optimised VWS and the random points, TRI values were extracted from the corresponding locations. With the aid of a one-tailed, non-parametric Mann–Whitney U test, the two sets of points were compared to determine whether the VWS occupied significantly flatter, lower-noise terrain profiles than the randomised points, at $\alpha = 0.05$.

Observational blind spot analysis

The virtual stations were then checked for operational utility through a blind spot analysis. A blind spot was defined as an area falling outside a 50 km radius of an active physical or virtual station. The 50 km threshold was used as it aligned with WMO guidelines for the spatial decorrelation scale of convective rainfall and regional synoptic stations (21). The total unmonitored area with only physical stations, and after the addition of VWS, was calculated to quantify the reduction in observational blind spots achieved through the MCDA.

Results

The spatial distribution of the 45 physical weather stations and 63 generated VWS is presented in Fig 2. Coordinates for the 45 physical stations and VWS are available in S1 and S2, respectively. The map also shows the virtual network suitability surface, which classified the study area based on suitability derived from the weighted combination of Normalised Terrain Ruggedness Index and proximity to water bodies, constrained by proximity to existing physical stations. The average distance to the nearest VWS was 59.68 km, while the maximum and minimum distances were 50.03 km and 130.33 km, respectively. The central parts of Zimbabwe, Southern Matabeleland North, and the southernmost parts had the highest virtual station placement suitability, while the eastern and parts of the northern regions were mostly unsuitable due to complex terrain. The results also show that the VWS were placed away from existing weather stations, as indicated by the physical station buffers.

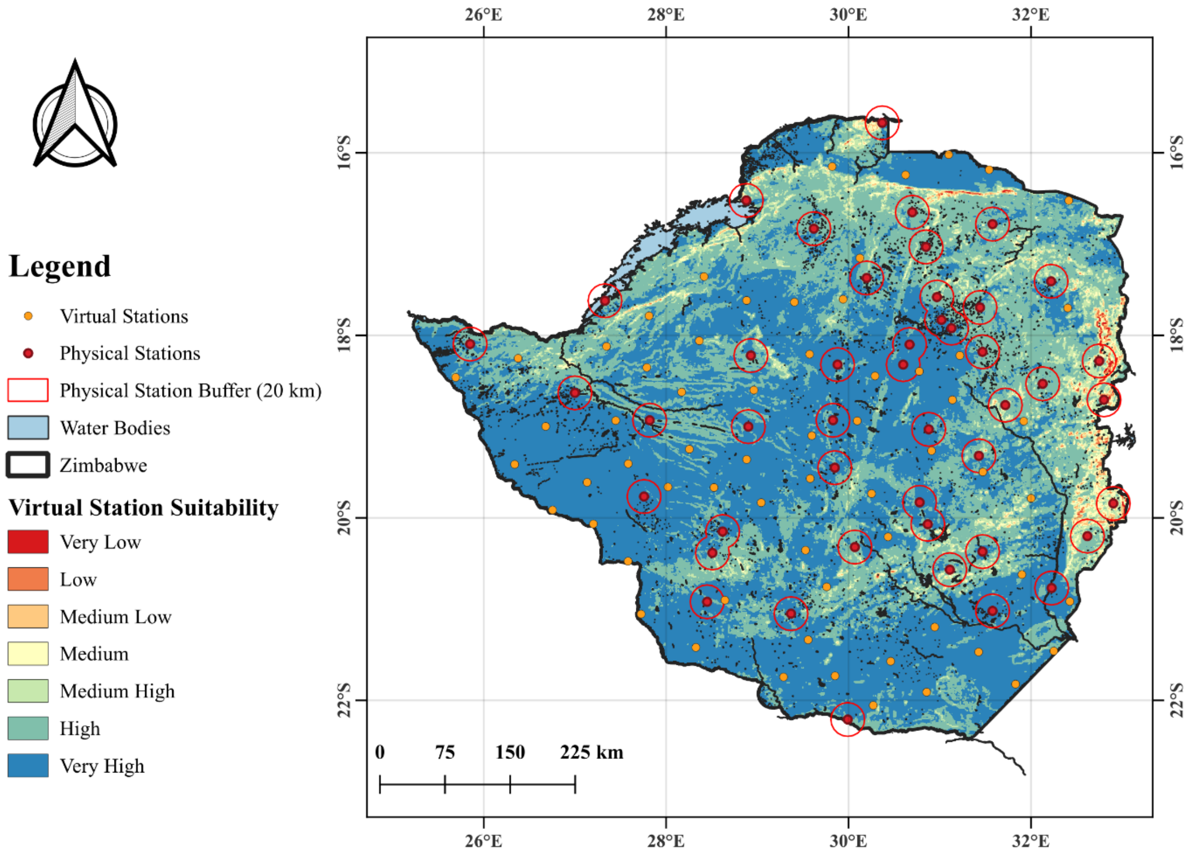

Fig 2. Virtual station suitability surface overlaid with virtual and physical station locations. Red buffer circles around physical stations indicate the distance from physical stations constraint applied to virtual station placement

Virtual station network representativeness

Fig 3 shows the distribution of virtual and physical stations relative to the total land area across Zimbabwe's AEZs. Regions IV and Va, which have the largest land area (approaching 30% each), had the highest number of virtual stations, n=19 and n=20, respectively. Regions I, IIa, and IIb had the lowest number of VWS, with n=0, n=1, and n=2, respectively, corresponding to their smaller land area. In contrast, the spatial distribution of physical stations was skewed toward Regions I, IIa, and IIb, although they are relatively smaller in geographic size. Conversely, the larger AEZs had a smaller number of observation infrastructure. For example, Region IV has approximately 30% of the land area but contains fewer physical stations (n=6) than the significantly smaller Region IIb (n=8).

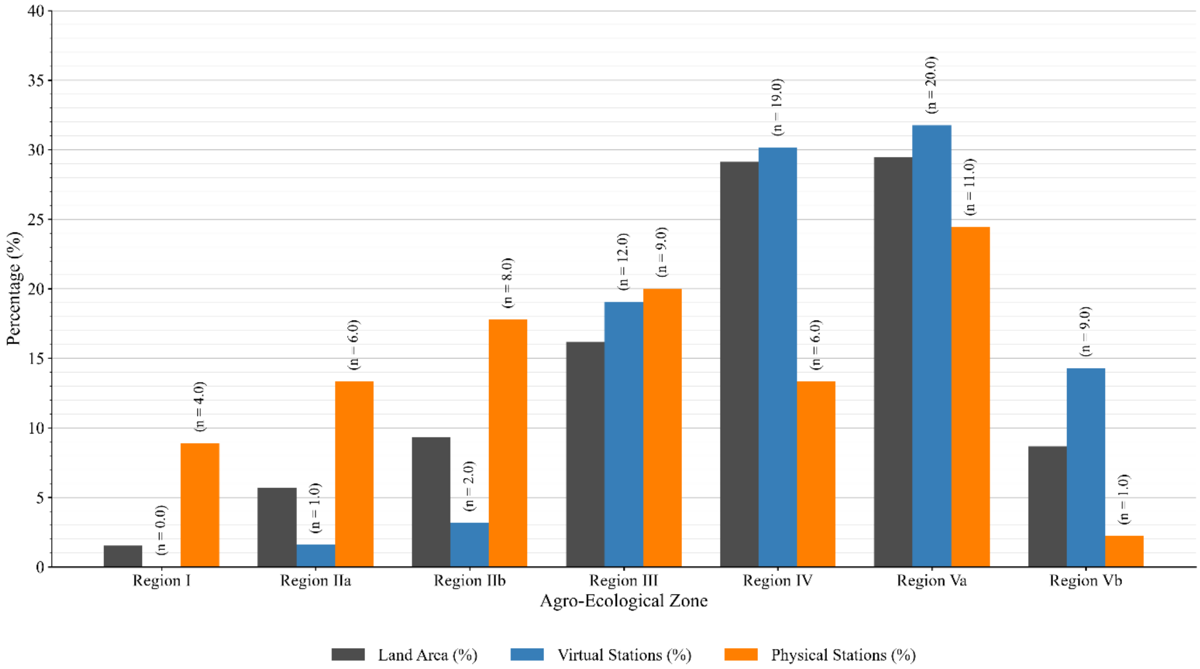

Fig 3. Distribution of virtual and physical stations across Agro-Ecological Zones, shown by percentage and station count (n)

Environmental constraint validation

Fig 4 shows a comparison of the TRI values extracted from the random control network and the optimised VWS network. The VWS network occupied areas with significantly lower TRI values, while the random network occupied areas with higher values, as shown by the narrow and wider interquartile ranges, respectively. Most of the TRI values for the VWS network were concentrated below 15 m, with a median of 9.33 m and a mean of 10.23 m. In contrast, the random network had significantly higher TRI values, with a much wider interquartile range. The mean TRI was 53.79 m, and the median was 29.82 m, with some random points exceeding 100 m and several outliers approaching 250 m. To test the significance of the differences in TRI across the 63 random points and 63 optimised stations, a Mann–Whitney U test was conducted, revealing a U-statistic of 425.00 and a p-value of 0.00.

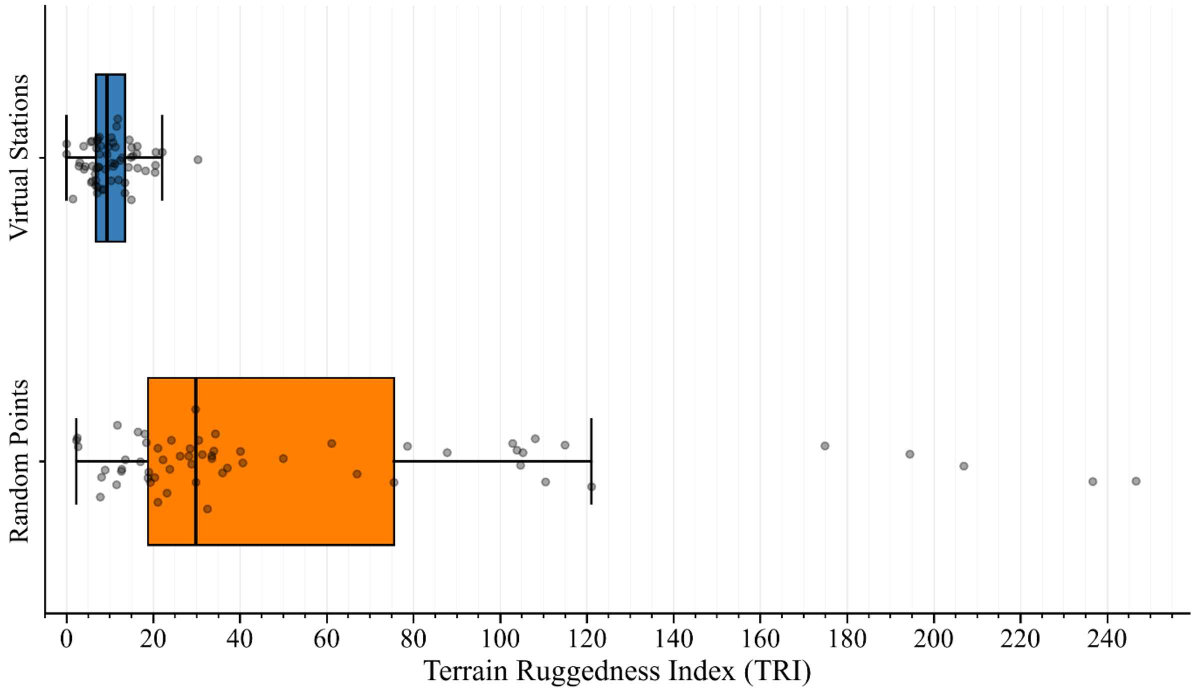

Fig 4. Boxplots of sampled Terrain Ruggedness Index values for random points and virtual weather stations

Blindspot analysis

Figs 5 and Fig 6 show the observational blind spots when the physical station network is used alone and when it is complemented with the VWS network, respectively. In Fig 6, the blind spots are significantly reduced, leaving mostly areas that would still be inaccessible for the deployment of physical stations due to complex terrain.

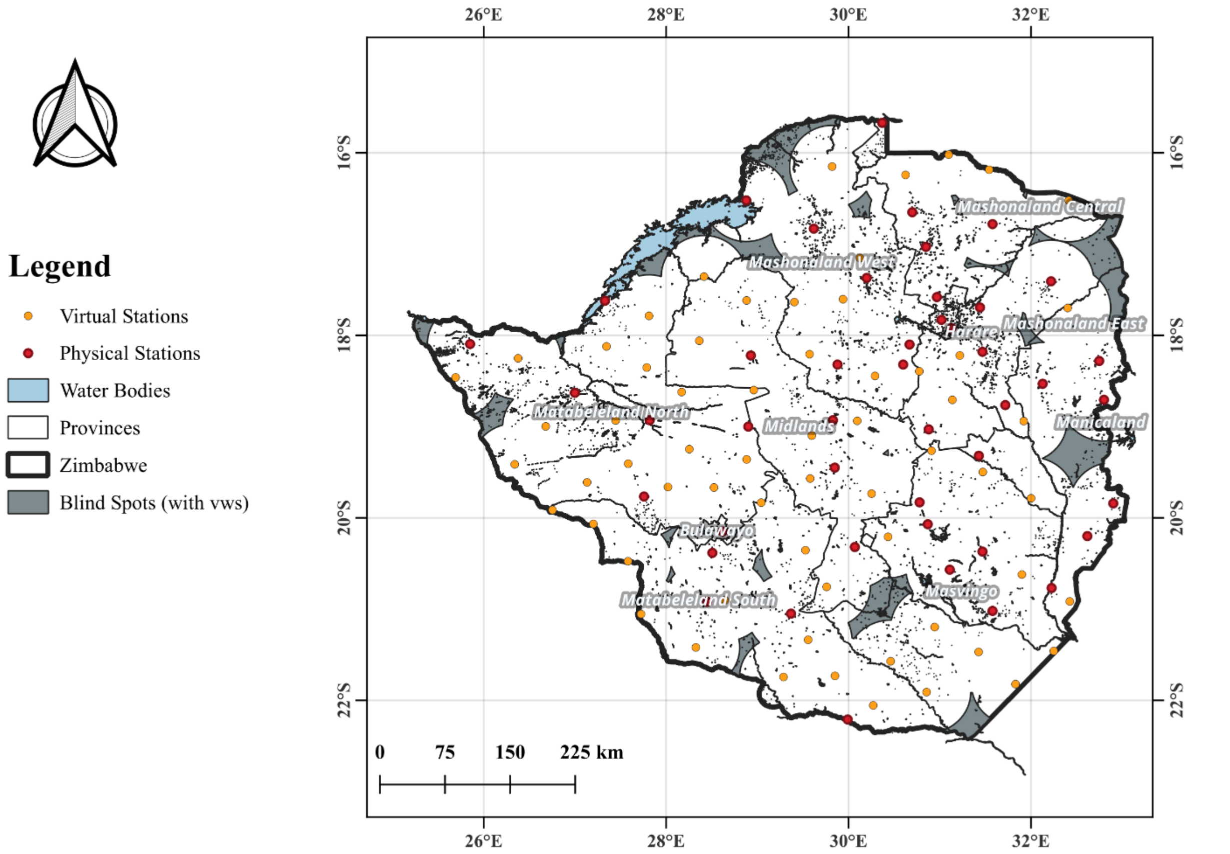

Fig 5. Observational blind spots based on the physical station network alone

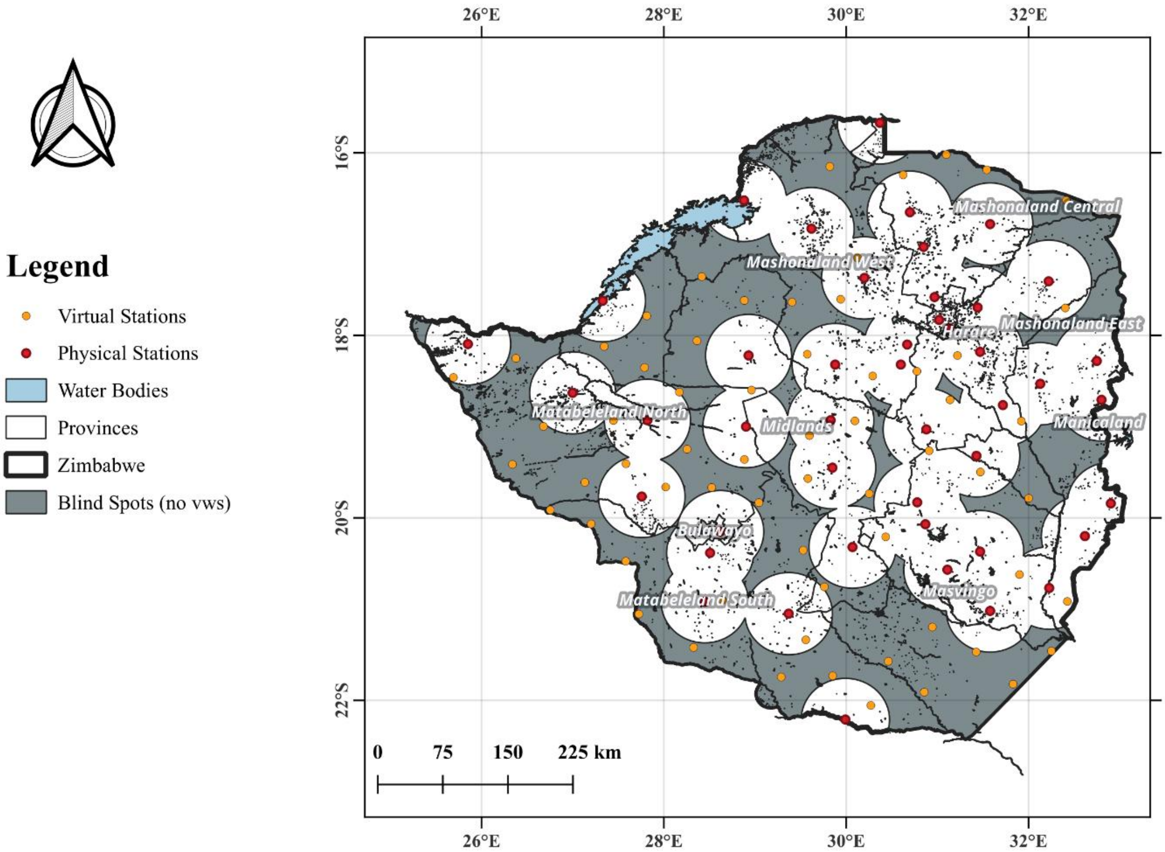

Fig 6. Observational blind spots after incorporating the virtual weather station network

Discussion

The VWS placement suitability observed in this study directly reflects the underlying terrain characteristics in Zimbabwe. High-suitability zones were concentrated in the central plateau, southern Matabeleland North, and the southernmost parts of the country. This reflects the gently undulating topography of those regions, which kept TRI values low. Conversely, parts of the north and most of the eastern highlands were unsuitable for VWS placement. This is consistent with the complexity of the terrain, both in altitude and undulation, as well as the presence of water bodies such as the Save and Odzi rivers and their tributaries. As highlighted by (22) mountainous regions pose a significant challenge for the placement of hydro-meteorological infrastructure, which can be extended to virtual stations, as they act as optimal places to extract data from satellite sources, in the context presented in this study. Hence, the same environmental factors that limit physical station density also constrain VWS placement.

This suggests that observational blind spots in environmentally complex zones are an artefact of both the siting methodology and the features of the landscape (23).

The VWS representativeness analysis provides clear evidence that the MCDA-optimised network has the potential to complement Zimbabwe's physical stations. Regions IV and Va, which account for 60% of the country's land area, had the largest allocation of virtual stations (39 out of 63 VWS combined), since the existing physical network is concentrated in Regions I, IIa, and IIb. Region IV draws attention, as it has only 6 physical stations despite holding 30% of the country's area. In contrast, Region IIb has 8 physical stations yet holds only 9.34% of the country's area. This mismatch aligns with historical station siting decisions, which favour accessible, economically prioritised, and higher-rainfall areas at the expense of larger, yet marginal, zones (24). The skewed network design is contrary to the optimal network design guidance provided by the WMO. For example, the WMO recommends station densities of 1 station per 600–900 km² in tropical areas, 1 station per 1,500–10,000 km² for arid regions, and 1 station per 25–100 km² for rugged terrain (21). By weighting VWS placement against existing physical observational infrastructure, the network offers a low-to-no-cost corrective mechanism that can improve representativeness in under-monitored zones. This approach has been applied in the Tekeze River basin in Ethiopia, proving effective in improving both the spatial distribution and the total count of observation points (25).

The effectiveness of the environmental constraints was also validated to confirm that the MCDA-optimised VWS placement approach performs meaningfully better than random placement. The VWS network occupied areas with an average TRI of 10.23 m and a median of 9.33 m. This contrasts with the random placement control experiment, which gave a mean of 53.79 m and a median of 29.82 m, significantly higher than the optimised placement. The Mann–Whitney U test performed on the TRI values extracted from the two groups confirmed that the difference was statistically significant and not due to chance, with $U=425$ and $p=0.00$.

Conclusion

Beyond confirming the results of the statistical test, the study has direct practical value. Sites with low TRI present conditions that are feasible for any future physical instruments, whether manual or conventional automatic weather stations. This means the VWS network is not merely an abstract suitability surface but identifies genuinely deployable locations. However, it is worth noting that proximity to water bodies and Terrain Ruggedness Index are only a few of several constraints that can be used for informed network design. Factors such as proximity to roads can also be included, though these are more important when siting physical infrastructure. Finally, the blind spot analysis shows a substantial reduction in blind spots once the VWS network is incorporated. Large areas of the country that would otherwise be unmonitored are now bridged by virtual observation points. The blind spots that remain in Fig 4b most likely represent locations where proximity to water bodies, high TRI, and existing physical station buffers all converge, making them the most difficult locations in which to allocate either physical or virtual infrastructure.

References

1. Liu Z -Q., Rabier F. The interaction between model resolution, observation resolution and observation density in data assimilation: A one-dimensional study. Quart J Royal Meteoro Soc. 2002 Apr;128(582):1367–86. doi:10.1256/003590002320373337

2. Gosset M, Dibi-Anoh PA, Schumann G, Hostache R, Paris A, Zahiri EP, et al. Hydrometeorological Extreme Events in Africa: The Role of Satellite Observations for Monitoring Pluvial and Fluvial Flood Risk. Surv Geophys. 2023 Feb;44(1):197–223. doi:10.1007/s10712-022-09749-6

3. Dunaieva I, Vecherkov V, Filina Y, Popovych V, Barbotkina E, Pashtetsky V, et al. Review of automatized meteorological stations use for agricultural purposes. IOP Conf Ser: Earth Environ Sci. 2021 Dec 1;937(3):032097. doi:10.1088/1755-1315/937/3/032097

4. WMO. Guide to Meteorological Instruments and Methods of Observation. 7th ed. Geneva, Switzerland: World Meteorological Organization; 2008. 681 p.

5. Gumindoga W, Rientjes THM, Haile AT, Makurira H, Reggiani P. Performance of bias-correction schemes for CMORPH rainfall estimates in the Zambezi River basin. Hydrol Earth Syst Sci. 2019 Jul 12;23(7):2915–38. doi:10.5194/hess-23-2915-2019

6. Baig F, Ali L, Faiz MA, Chen H, Sherif M. From bias to accuracy: Transforming satellite precipitation data in arid regions with machine learning and topographical insights. Journal of Hydrology. 2025 Jun;653:132801. doi:10.1016/j.jhydrol.2025.132801

7. Polina K. The Evolution and Impact of Virtual Stations. Blue Water Intelligence (BWI) [Internet]. 2024 Feb 6 [cited 2026 May 13]. Available from: https://bwi.earth/the-evolution-and-impact-of-virtual-stations/

8. Franco BM, Hernández-Callejo L, Navas-Gracia LM. Virtual weather stations for meteorological data estimations. Neural Comput & Applic. 2020 Aug;32(16):12801–12. doi:10.1007/s00521-020-04727-8

9. Maviza A, Ahmed F. Climate change/variability and hydrological modelling studies in Zimbabwe: a review of progress and knowledge gaps. SN Appl Sci. 2021 May;3(5):549. doi:10.1007/s42452-021-04512-9

10. Tan J, Petersen WA, Tokay A. A Novel Approach to Identify Sources of Errors in IMERG for GPM Ground Validation. Journal of Hydrometeorology. 2016 Sep 1;17(9):2477–91. doi:10.1175/JHM-D-16-0079.1

11. FAO. Country profile - Zimbabwe. FAO AQUASTAT Reports [Internet]. Food and Agriculture Organization of the United Nations. Italy, Rome; 2016 [cited 2026 May 18]. p. 21. Available from: https://openknowledge.fao.org/server/api/core/bitstreams/b43602b2-724e-45ed-8861-727d0381b66e/content

12. Gutierrez SRM, Fenta AA, Meshesha TM, Belay AS. Unveiling the Accuracy of New-Generation Satellite Rainfall Estimates across Bolivia's Complex Terrain. Remote Sensing. 2024 Jun 18;16(12):2211. doi:10.3390/rs16122211

13. Waller J, Ballard S, Dance S, Kelly G, Nichols N, Simonin D. Diagnosing Horizontal and Inter-Channel Observation Error Correlations for SEVIRI Observations Using Observation-Minus-Background and Observation-Minus-Analysis Statistics. Remote Sensing. 2016 Jul 8;8(7):581. doi:10.3390/rs8070581

14. MSDZ. Meteorological Services Department of Zimbabwe. Your weather and climate services for a resilient future [Organisation] [Internet]. Harare, Zimbabwe; 2026 [cited 2026 Apr 28]. Available from: https://www.weatherzw.org.zw/

15. OpenTopography. Shuttle Radar Topography Mission (SRTM) Global [Internet]. OpenTopography; 2013 [cited 2026 May 18]. Available from: https://opentopography.org/meta/OT.042013.4326.1 doi:10.5069/G9445JDF

16. OCHA. Zimbabwe: Waterways (OpenStreetMap Export) | Humanitarian Dataset | HDX [Internet]. United Nations Office for the Coordination of Humanitarian Affairs; 2026 [cited 2026 May 18]. Available from: https://data.humdata.org/dataset/hotosm_zwe_waterways

17. Manatsa D, Mushore D Terence, Gwitira I, Chemura A, Shekede M Davis, Mugandani R, et al. Revision Of Zimbabwe's Agro-Ecological Zones [Revision Report] [Internet]. Zimbabwe: Zimbabwe National Geospatial and Space Agency

(ZINGSA); 2020 Sep [cited 2026 May 23]. p. 113. Revision Report no.: 1. Available from: https://www.researchgate.net/profile/Desmond-Manatsa/publication/347966377_Report_on_Revised_Agroecological_Zones_of_Zimbabwe_in_press/links/5feab23c299bf140885658b2/Report-on-Revised-Agroecological-Zones-of-Zimbabwe-in-press.pdf?origin=publication_detail&_tp=eyJjb250ZXh0Ijp7ImZpcnN0UGFnZSI6InB1YmxpY2F0aW9uIiwicGFnZSI6InB1YmxpY2F0aW9uRG93bmxvYWQiLCJwcmV2aW91c1BhZ2UiOiJwdWJsaWNhdGlvbiJ9fQ

18. Trevisani S, Teza G, Guth PL. Hacking the topographic ruggedness index. Geomorphology. 2023 Oct;439:108838. doi:10.1016/j.geomorph.2023.108838

19. Xu J, Liu Z. Machine learning-based retrieval of total column water vapor over land using GMI-sensed passive microwave measurements. GIScience & Remote Sensing. 2024 Aug 5;61(1):2385180. doi:10.1080/15481603.2024.2385180

20. Saaty RW. The analytic hierarchy process—what it is and how it is used. Mathematical Modelling. 1987;9(3–5):161–76. doi:10.1016/0270-0255(87)90473-8

21. WMO. Guide to Meteorological Instruments and Methods of Observation. 2024th ed. Vol. 3. Geneva: World Meteorological Organization; 2023. 529 p. (Observing Systems; no. 8).

22. Suri A, Azad S. Optimal placement of rain gauge networks in complex terrains for monitoring extreme rainfall events: a review. Theor Appl Climatol. 2024 Apr;155(4):2511–21. doi:10.1007/s00704-024-04856-3

23. Mauger GS, Bumbaco KA, Hakim GJ, Mote PW. Optimal design of a climatological network: beyond practical considerations. Geosci Instrum Method Data Syst. 2013 Jul 22;2(2):199–212. doi:10.5194/gi-2-199-2013

24. Maganga T, Conrad Suso C. The impact of colonial and contemporary land policies on climate change adaptation in Zimbabwe's communal areas. Jàmbá. 2022 Oct 28;14(1). doi:10.4102/jamba.v14i1.1311

25. Teklеyohannes M, Grum B, Abebe N, Abebe BA. Optimization of rain gauge network using multi-criteria decision analysis and entropy approaches: case of Tekeze River basin, northwestern Ethiopia. Theor Appl Climatol. 2021 Jul;145(1–2):159–74. doi:10.1007/s00704-021-03604-1

Supporting information

S1 File.

S2 File.